

# Weighted-Sum Energy Efficiency Maximization in User-Centric Uplink Cell-Free Massive MIMO

Donghwi Kim, *Graduate Student Member, IEEE*, Liesbet Van der Perre, *Senior Member, IEEE*, and Wan Choi, *Fellow, IEEE*

**Abstract**—This paper introduces the weighted-sum energy efficiency (WSEE) as an advanced performance metric designed to represent the uplink energy efficiency (EE) of individual user equipment (UE) in a user-centric Cell-Free massive MIMO (CF-mMIMO) system more accurately. In this realistic user-centric CF-mMIMO context, each UE may exhibit distinct characteristics, such as maximum transmit power limits or specific minimum data rate requirements. By computing the EE of each UE independently and adjusting the weights accordingly, the system can accommodate these unique attributes, thus promoting energy-efficient operation. The uplink WSEE is formulated as a multiple-ratio fractional programming (FP) problem, representing a weighted sum of the EE of individual UEs, which depends on each UE's transmit power and the combining vector at the CPU. To effectively maximize WSEE, we present optimization algorithms that utilize the Dinkelbach transform and the quadratic transform (QT). Applying the QT twice consecutively yields significant performance gains in terms of WSEE. This framework establishes a foundation for developing operational strategies tailored to specific system requirements.

**Index Terms**—Cell-free massive MIMO, user-centric association, weighted-sum energy efficiency (WSEE), fractional programming, quadratic transform

## I. INTRODUCTION

THE increasing demand for data transmission rates and volumes remains a major challenge in modern wireless communication systems [1]. To achieve high data rates while maintaining quality of service (QoS) across numerous wireless devices, massive multiple-input multiple-output (MIMO) architectures have been standardized as a key 5G technology and widely adopted. Among various massive MIMO architectures, network or distributed MIMO utilizes a spatially distributed set of antennas to cooperatively reduce inter-cell interference in traditional cellular systems, allowing for higher data rates [2].

An advanced form of Network MIMO, known as cell-free massive MIMO (CF-mMIMO), has garnered considerable attention in recent years [3]. In CF-mMIMO systems, a large number of distributed access points (APs) are connected to a central processing unit (CPU) via backhaul links. This configuration supports collaborative communication, enabling multiple user equipments (UEs) to share the same time-frequency resources. The spatially distributed architecture

of CF-mMIMO offers additional macro-diversity gains from dense AP deployment and improves fairness among UEs.

In recent CF-mMIMO literature, the user-centric model has emerged as a highly promising system implementation approach. In this model, each UE is served by a subset of APs rather than by all APs [4], [5]. Configuring the AP subset in a user-centric CF-mMIMO network allows for significant scalability improvements, optimizing computational complexity with minimal performance loss compared to the original CF-mMIMO. In user-centric CF-mMIMO, the CPU processes signals from APs based on the configured AP-UE associations, constructing AP subsets as per the chosen association scheme. To maximize network sum spectral efficiency (SE), an effective signal processing method involves applying appropriate weights to the signals gathered from each AP, thereby enhancing the SE for each UE. This technique, known as large-scale fading decoding (LSFD) [6], is highly effective. While the user-centric approach reduces computational overhead, CF-mMIMO inherently encounters complex interference among UEs. Consequently, an efficient resource allocation strategy is essential for managing interference and ensuring fair service for a large user base. In this regard, optimal power control is crucial to achieving high performance in CF-mMIMO systems [7]–[9].

As network density and the number of UEs continue to increase, energy efficiency (EE) has become as crucial as SE [10]–[12]. While SE indicates the efficiency of data transmission, EE measures the efficient operation of the entire system. Thus, a primary goal in next-generation wireless communication systems is to maximize EE while maintaining adequate SE. The conventional global EE (GEE) is defined as the ratio of the total data transmission rate to the total power consumption, representing the amount of data transmitted per unit of energy used [13]. In time-division duplex (TDD) wireless communication systems, EE can be evaluated separately for the uplink and downlink phases, each influenced by how the system's power consumption is calculated.

Power consumption can be divided into two main components: network-side power [14], which is used by network elements such as the AP and backhaul, and UE-side power [15], which includes the power needed for transmission, reception, and circuit operations within the device. In the downlink, network-side power consumption is the primary consideration, as the network manages the AP's transmit power to serve multiple UEs. Conversely, in the uplink, the data transmission rate relies on each UE's transmit power, making UE-side power consumption a critical factor.

D. Kim and W. Choi are with the Department of Electrical and Computer Engineering, and the Institute of New Media and Communications, Seoul National University (SNU), Seoul 08826, Korea (e-mail: yob0322@snu.ac.kr; wanchoi@snu.ac.kr). (*Corresponding Author: Wan Choi*)

L. Van der Perre is with ESAT-WaveCore, KU Leuven, Ghent, Belgium. (e-mail: liesbet.vanderperre@kuleuven.be).

Previous studies on the EE of CF-mMIMO systems have mainly focused on downlink global energy efficiency (DL-GEE), defined as the ratio of the total downlink data transmission rate to total network power consumption [16]–[19]. In contrast, there has been limited research addressing the uplink EE in CF-mMIMO systems. In [20], large-scale fading processing (LSFP) methods were proposed to maximize the GEE for both uplink and downlink. However, these methods relied on heuristic algorithms for power allocation. The work in [21] proposed a method to define uplink global energy efficiency (UL-GEE) when quantization occurs at the APs. It optimized the uplink transmit power using successive convex approximation (SCA) and sub-optimal geometric programming (GP). Another work [22] proposed a power control strategy aimed at maximizing max-min fairness in the energy efficiencies of individual UEs, rather than focusing on GEE. The latest study [23] examined the quantization bits and UE transmit power required to optimize UL-GEE in uplink CF-mMIMO with low-resolution ADCs. Since these studies focused on GEE or EE for the UE with the worst performance, addressing the EEs of individual UEs separately remains challenging.

Departing from the conventional GEE, our primary focus is on the EE of individual UEs, defined as the ratio of each UE's SE to its power consumption. Specifically, we utilize the weighted-sum energy efficiency (WSEE) as our key performance metric, incorporating weights that reflect each UE's unique characteristics, such as power budget and data rate requirements. The WSEE metric is particularly suited for multi-user systems, as it allows for prioritization among UEs by adjusting their individual weights.

The proposed WSEE is defined as the weighted sum of the EE of individual UEs. This provides flexibility to reflect the unique requirements and priorities of each UE, which cannot be addressed in the overall power consumption compared to the simple total transmission rate. For instance, if a specific UE temporarily demands a high data rate or is limited in power usage, a larger weight may be given to that UE to preferentially improve the EE of that UE. Furthermore, it is possible to separate UEs into several groups and manage EE for each UE group more strictly by appropriately adjusting the weights. WSEE can effectively balance the two goals of optimizing the EE of the entire network and meeting the requirements for each UE. In addition, the proposed WSEE can control the power use of each UE particularly effectively, focusing on the power consumption on the UE-side, thereby extending battery life and contributing to reducing energy costs. This can enhance the reliability and lifetime of the link in important communication situations. The EE of each UE in the uplink WSEE is significantly affected by not only its own transmit power but also the power control of other UEs in the system. To address this, we propose an energy-efficient power control and distributed signal processing framework suitable for uplink user-centric CF-mMIMO systems.

The main contributions of this paper are summarized as below.

- Our work is the first to analyze uplink WSEE in CF-mMIMO systems. We propose the new metric of uplink WSEE, which allows for comprehensive evaluations of

uplink EE with various priorities of UEs. We also maximize the proposed WSEE by optimizing each UE's uplink transmit power and the LSFD combining vector at the CPU, once all UEs' weights and AP-UE associations are determined.

- The WSEE maximization problem that we aim to solve is a non-concave fractional and NP-hard problem. To convert the WSEE into an tractable form, we leverage the Dinkelbach transform [24], [25] and quadratic transform (QT) [26] from fractional programming (FP). We derive two algorithms, one is based on the Dinkelbach-like transform, applying the Dinkelbach transform individually to each UE's EE. The other is based on QT, which is applied to both each UE's EE and their SINR. In particular, the QT-based alternating optimization (AO) proposed in this paper theoretically guarantees convergence by solving subproblems that are concave or can be optimized globally at each iteration. This contributes to a significant improvement in network performance by enabling fast and stable optimization in practical network operations. The proposed algorithms are all based on AO and share the same computational complexity, but have different convergence rates depending on the transform used in FP.
- We design the WSEE optimization problem to incorporate each UE's maximum power limit and minimum data rate requirements. Traditional GEE-focused approaches prioritize overall network efficiency, so there are limitations in ensuring the performance of individual UEs because the performance degradation of a particular UE may be offset by the performance improvement of another UE. The proposed WSEE optimization method can prevent the problem of performance degradation or even convergence to zero for some UE, which can occur in the GEE optimization. Simulation results highlight the performance distribution across UEs, emphasizing the differences between the two approaches and demonstrating the effectiveness of the proposed method.

### A. Outline

The remainder of this paper is organized as follows. Section II describes the uplink user-centric CF-mMIMO system model. Section III defines the uplink EE of individual UE and the WSEE metric based on the uplink EE. Additionally, we present the weighted-global energy efficiency (WGEE) as a comparative metric for WSEE. In Section IV, we formulate the WSEE and WGEE maximization problems and solve corresponding the optimization problems. To achieve this, we develop algorithms based on Dinkelbach transform and QT respectively. Section VI provides a comprehensive performance evaluation of the proposed algorithms under various weight conditions. Finally, Section VII concludes the paper.

### B. Notations

For a scalar  $x$ , superscript  $x^\dagger$  denotes the complex conjugate. For a vector  $\mathbf{a}$  and a matrix  $\mathbf{A}$ , superscript  $(\cdot)^H$  denotes the Hermitian.  $\|\mathbf{a}\|$ ,  $\text{tr}(\mathbf{A})$  and  $\text{diag}(\mathbf{a})$  are used as the

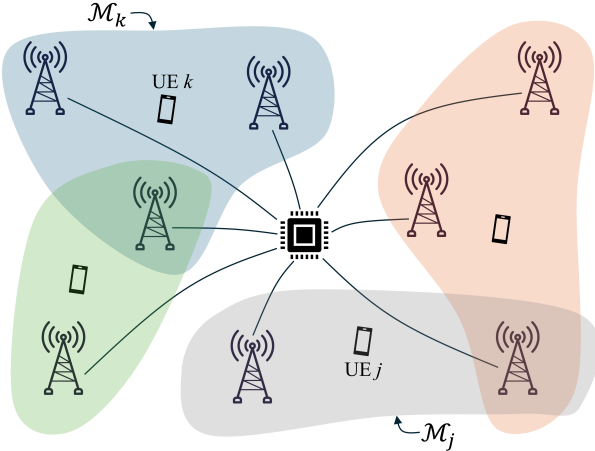


Fig. 1: Illustration of a user-centric CF-mMIMO system

Euclidean norm of  $\mathbf{a}$ , the trace of  $\mathbf{A}$ , and the diagonal matrix whose diagonal elements are  $\mathbf{a}$ , respectively.  $\mathbf{I}_N$  and  $\mathbf{0}_N$  are identity and zero matrices. For a set  $\mathcal{S}$ ,  $|\mathcal{S}|$  is the cardinality of  $\mathcal{S}$ . The expression  $\mathcal{S} \setminus \{s\}$  stands for the rest of the set except for the element  $s$ . Also,  $\mathbb{E}\{\cdot\}$  means the expectation.

## II. SYSTEM MODEL

We consider a CF-mMIMO system with  $M$  APs, each equipped with  $N$  antennas. There are  $K$  single antenna UEs, randomly distributed across a wide area. To benefit from the favorable propagation and channel hardening effects of CF-mMIMO, we assume that  $MN \gg K$ . We adopt a user-centric approach [4], where all APs are connected to the CPU via ideal backhaul, but each AP only serves a subset of UEs. The system model is depicted in Fig. 1. The subset of APs serving UE  $k$  is denoted as  $\mathcal{M}_k \subseteq \{1, \dots, M\}$ , and the subset of UEs served by AP  $m$  is denoted as  $\mathcal{D}_m \subseteq \{1, \dots, K\}$ . TDD is adopted to enable both uplink and downlink transmissions on the same frequency band. This analysis focuses on uplink channel estimation and uplink data transmission, excluding downlink transmission. We adopt a block fading channel model, where each coherence block has a length of  $\tau_c$  (in samples). During each coherence interval, all UEs transmit pilot sequences in the first  $\tau_p$  samples, while the remaining  $\tau_c - \tau_p$  samples are allocated for uplink data transmission. After uplink channel estimation, the CPU uses the optimized parameters to control the uplink power of each UE. For simplicity, we assume that the UEs instantly know the optimized parameters, meaning time required for downlink transmission of these parameters is negligible. We consider a Rayleigh fading vector channel model, where the channel coefficient vector  $\mathbf{g}_{mk} \in \mathbb{C}^{N \times 1}$  between AP  $m$  and UE  $k$  follows  $\mathbf{g}_{mk} \sim \mathcal{CN}(\mathbf{0}, \beta_{mk} \mathbf{I}_N)$ . Here,  $\beta_{mk}$  represents the large-scale fading coefficient determined by the distance and propagation environment. The value of  $\beta_{mk}$ , representing path loss and shadowing, varies slowly compared to the small-scale fading coefficients. It is assumed that the large-scale fading coefficients  $\beta_{mk}$  are known to APs  $m \in \{1, \dots, M\}$ .

### A. AP-UE Association

Each UE can select its serving AP cluster  $\mathcal{M}_k$  based on the large-scale fading information available to it. We use the largest-large-scale-fading-based selection method, where UE  $k$  selects the top  $|\mathcal{M}_k|$  APs with the best channel conditions. Specifically, the APs in  $\mathcal{M}_k$  satisfy the following condition,

$$\sum_{m=1}^{|\mathcal{M}_k|} \frac{\bar{\beta}_{mk}}{\sum_{m'=1}^M \beta_{m'k}} \geq \delta, \quad (1)$$

where  $\bar{\beta}_{1k}, \dots, \bar{\beta}_{Mk}$  are the sorted large-scale fading coefficients in descending order, and  $\delta$  is a parameter between 0 and 1 that indirectly controls the size of the AP cluster serving each UE. Based on the determined association  $\mathcal{M}_k$ , we define the block-diagonal matrix  $\mathbf{D}_k = \text{diag}(\mathbf{D}_{1k}, \dots, \mathbf{D}_{Mk})$ , where  $\mathbf{D}_{mk} = \mathbf{I}_N$  if  $m \in \mathcal{M}_k$ , and  $\mathbf{D}_{mk} = \mathbf{0}_N$  otherwise.

### B. Uplink Channel Estimation

During the channel estimation phase, all UEs transmit their pilot sequences, and each AP  $m$  locally estimates the channels of UEs in its subset  $\mathcal{D}_m$ . UE  $k$  uses the orthogonal pilot sequence matrix  $\Phi \in \mathbb{C}^{\tau_p \times K}$ , where the column  $\phi_k$  is the pilot sequence for UE  $k$ . If  $K \leq \tau_p$ , all UEs can use mutually orthogonal pilot sequences. However, in general,  $\tau_p \ll K$ , leading to pilot contamination. In this scenario, let  $\mathcal{P}_k$  represent the set of UEs sharing the same pilot sequence as UE  $k$ . The signal received by AP  $m$  is given by

$$\mathbf{y}_m^{\text{pilot}} = \sqrt{\tau_p \rho_p} \sum_{k=1}^K \mathbf{g}_{mk} \phi_k^H + \mathbf{n}_m^{\text{pilot}}, \quad (2)$$

where  $\rho_p$  represents the uplink transmit signal-to-noise ratio (SNR) of the pilot symbols, normalized by the noise power  $N_0 = \sigma_{\text{ul}}^2$ . The term  $\mathbf{n}_m^{\text{pilot}}$  denotes the received noise, with each element independently and identically distributed (i.i.d.) as  $\mathcal{CN}(0, 1)$ . The minimum mean-squared error (MMSE) estimate of  $\mathbf{g}_{mk}$  is given by

$$\hat{\mathbf{g}}_{mk} = \frac{\sqrt{\tau_p \rho_p} \beta_{mk}}{\tau_p \rho_p \sum_{k' \in \mathcal{D}_m} \beta_{mk'} |\phi_{k'}^H \phi_k|^2 + 1} \tilde{\mathbf{y}}_m^{\text{pilot}}, \quad (3)$$

where

$$\begin{aligned} \tilde{\mathbf{y}}_m^{\text{pilot}} &= \mathbf{y}_m^{\text{pilot}} \phi_k \\ &= \sqrt{\tau_p \rho_p} \mathbf{g}_{mk} + \sqrt{\tau_p \rho_p} \sum_{k' \neq k} \mathbf{g}_{mk'} \phi_{k'}^H \phi_k + \mathbf{n}_m^{\text{pilot}} \phi_k. \end{aligned} \quad (4)$$

From the i.i.d. property of small-scale fading and noise, the channel estimate  $\hat{\mathbf{g}}_{mk}$  also consists of  $N$  i.i.d. Gaussian components. For convenience, we define  $\gamma_{mk}$  as the mean-square value of a single component of  $\hat{\mathbf{g}}_{mk}$ , which is given by

$$\gamma_{mk} = \frac{\tau_p \rho_p \beta_{mk}^2}{\tau_p \rho_p \sum_{k' \in \mathcal{P}_k} \beta_{mk'} |\phi_{k'}^H \phi_k|^2 + 1}. \quad (5)$$

### C. Uplink Data Transmission

In the distributed operation of user-centric CF-mMIMO, signal processing is divided between the AP and the CPU [6]. During the uplink transmission phase, all UEs transmit signals to the APs. The signal received by AP  $m$  is given by

$$\mathbf{y}_m^{\text{ul}} = \sum_{k=1}^K \mathbf{g}_{mk} x_k + \mathbf{n}_m, \quad (6)$$

where the transmitted signal  $x_k = \sqrt{q_k} s_k$  has a power  $q_k$ , with  $s_k$  being the normalized transmit signal such that  $\mathbb{E}\{|s_k|^2\} = 1$ . Each AP  $m$  uses a local maximum ratio combining (MRC) vector  $\mathbf{v}_{mk} = \mathbf{D}_{mk} \hat{\mathbf{g}}_{mk}$ , the natural counterpart to conjugate beamforming used in downlink CF-mMIMO literature. The local estimate of the signal  $x_k$  transmitted by UE  $k$  at AP  $m$  is given by

$$\hat{x}_{mk} = \mathbf{v}_{mk}^H \mathbf{D}_{mk} \mathbf{y}_m^{\text{ul}} = \hat{\mathbf{g}}_{mk}^H \mathbf{D}_{mk} \mathbf{y}_m^{\text{ul}}. \quad (7)$$

After local data estimation at the APs, the local estimates are forwarded to the CPU via backhaul links. The CPU then completes the final data decoding for each UE as follows:

$$\hat{x}_k = \sum_{m=1}^M u_{mk}^\dagger \hat{x}_{mk} = \sum_{m=1}^M u_{mk}^\dagger \hat{\mathbf{g}}_{mk}^H \mathbf{D}_{mk} \mathbf{y}_m^{\text{ul}}, \quad (8)$$

where  $u_{mk} \in \mathbb{C}$  is the weight applied by the CPU to the local estimate  $\hat{x}_{mk}$ . This process is known as large-scale fading decoding (LSFD). The CPU applies the LSFD matrix  $\mathbf{U} \in \mathbb{C}^{M \times K}$ , where the  $k^{\text{th}}$  column  $\mathbf{u}_k \in \mathbb{C}^{M \times 1}$  represents the LSFD combining vector for UE  $k$ .

Substituting (6) into the above expression and performing some simple mathematical manipulations, the final estimated result  $\hat{x}_k$  can be decomposed into the terms of desired signal  $\text{DS}_k$ , beamforming uncertainty gain  $\text{BU}_k$ , inter-user interference  $|\text{UI}_{kk'}|$ , and effective noise  $\text{EN}_k$ , respectively, as

$$\begin{aligned} \hat{x}_k &= \mathbb{E} \left[ \underbrace{\sum_{m=1}^M u_{mk}^\dagger \hat{\mathbf{g}}_{mk}^H \mathbf{D}_{mk} \mathbf{g}_{mk}}_{(\text{DS}_k, \text{desired signal})} \right] x_k \\ &+ \underbrace{\left( \sum_{m=1}^M u_{mk}^\dagger (\hat{\mathbf{g}}_{mk}^H \mathbf{D}_{mk} \mathbf{g}_{mk} - \mathbb{E}\{\hat{\mathbf{g}}_{mk}^H \mathbf{D}_{mk} \mathbf{g}_{mk}\}) \right)}_{(\text{BU}_k, \text{beamforming uncertainty})} x_k \\ &+ \sum_{k' \neq k} \underbrace{\left( \sum_{m=1}^M u_{mk}^\dagger \hat{\mathbf{g}}_{mk}^H \mathbf{D}_{mk} \mathbf{g}_{mk'} \right)}_{(|\text{UI}_{kk'}|, \text{inter-user interference})} x_{k'} \\ &+ \underbrace{\sum_{m=1}^M u_{mk}^\dagger \hat{\mathbf{g}}_{mk}^H \mathbf{D}_{mk} \mathbf{n}_m}_{(\text{EN}_k, \text{effective noise})}. \end{aligned} \quad (9)$$

Now, based on the previous discussion, the SE of UE  $k$  can be described in closed form, as detailed in the following lemma.

**Lemma 1.** [27, Chapter 5] *In a user-centric CF-mMIMO system with local MRC and LSFD combiner, the uplink SE of UE  $k$  can be expressed as*

$$\text{SE}_k^{\text{ul}} = \frac{\tau_c - \tau_p}{\tau_c} \log_2 \left( 1 + \text{SINR}_k^{\text{ul}} \right), \quad (10)$$

and  $\text{SINR}_k^{\text{ul}}$  is given by (11) and (12) at the bottom of the next page.

Note that both of the numerator and the denominator of the  $\text{SINR}_k^{\text{ul}}$  are affine functions with respect to  $\mathbf{q}$ . In Lemma 1, given the channel statistics, the SINR of UE  $k$  depends on both  $\mathbf{u}_k$  and  $\mathbf{q}$ . When  $\mathbf{q}$  is held constant, the SINR reduces to a generalized Rayleigh quotient with respect to  $\mathbf{u}_k$ . It is also well known that  $\mathbf{u}_k$ , which maximizes this form of SINR, can be derived in closed form [28]. For our system model, the optimal  $\mathbf{u}_k$  is computed as

$$\mathbf{u}_k = q_k \mathbf{\Gamma}^{-1} \mathbb{E}\{\hat{\mathbf{g}}_{mk}^H \mathbf{D}_{mk} \mathbf{g}_{mk}\}, \quad (13)$$

where

$$\begin{aligned} \mathbf{\Gamma} &= \sum_{k' \neq k} q_{k'} \mathbb{E}\left\{ \left| \hat{\mathbf{g}}_{mk}^H \mathbf{D}_{mk} \mathbf{g}_{mk'} \right|^2 \right\} \\ &+ \sigma_{\text{ul}}^2 \text{diag} \left( \mathbb{E}\left\{ \left| \hat{\mathbf{g}}_{1k}^H \mathbf{D}_{1k} \right|^2 \right\}, \dots, \mathbb{E}\left\{ \left| \hat{\mathbf{g}}_{Mk}^H \mathbf{D}_{Mk} \right|^2 \right\} \right) \\ &+ \tilde{\mathbf{D}}_k \end{aligned} \quad (14)$$

where  $\tilde{\mathbf{D}}_k$  is the matrix obtained by replacing each block of  $\mathbf{D}_k$  with its complement matrix.

## III. PERFORMANCE METRICS

### A. Energy Efficiency of Each User

Before defining the WSEE, we first define the EE of individual UEs as [29]:

$$\text{EE}_k = \frac{B \cdot \text{SE}_k^{\text{ul}}}{P_k}, \quad (15)$$

where  $B$  is the bandwidth. In (15),  $P_k$  represents the power consumed by UE  $k$  to achieve the corresponding  $\text{SE}_k^{\text{ul}}$ . In typical DL-GEE analysis, the total network power consumption accounts for the power consumed by distributed APs and backhuls [30]. In contrast, in this UL study, we focus solely on the power consumed by the UE, excluding the power drawn by the APs, backhaul, and CPU.

Then, the power consumption model for UE  $k$  can be expressed as

$$P_k = P_{\text{UE},k} = P_{\text{TX},k} + P_{\text{CP},k}, \quad (16)$$

where  $P_{\text{TX},k}$  is the uplink transmit power of the UE, and  $P_{\text{CP},k}$  is the circuit power consumed by the UE's hardware. The transmit signal power  $P_{\text{TX},k}$  after power amplifier (PA), proportional to the transmit signal power  $q_k$ , is given by

$$P_{\text{TX},k} = \frac{1}{\zeta_k} q_k, \quad (17)$$

where  $\zeta_k$  is the PA efficiency of UE  $k$ , and  $q_k$  is a value having an upper limit of the maximum transmission signal power  $p_{\text{max},k}$ .  $P_{\text{CP},k}$  is the power consumed to drive the circuit elements of UE  $k$ , including cooling, power supply,

control signaling, etc. This value is determined by the UE hardware configuration, but may be regarded as a fixed value in an uplink transmission.

**Remark.** The metric  $EE_k$ , defined by (15) – (17), represents the amount of power  $P_k$  that must be consumed by UE  $k$  in a user-centric CF-mMIMO system to achieve the desired uplink data rate  $B \cdot SE_k^{\text{ul}}$ . Among the factors influencing  $P_k$ , the only parameter that a UE can directly adjust is its transmit power. In the case of  $SE_k$ , it is determined by both the transmit power of each UE and the LSFD combiner at the CPU. The network is responsible for jointly optimizing the transmit power and LSFD combiner. Based on the AP-UE association and the channel information obtained from the APs, the CPU can determine  $\mathbf{q}$  and  $\mathbf{U}$ . Subsequently, downlink control signals can be used to instruct each UE on its transmit power. The UEs then perform uplink data transmission using the power levels received from the network. This operation is ensured by the performance guarantees provided through the TDD block fading channel model.

### B. Weighted-Sum Energy Efficiency

We introduce the WSEE as an uplink performance metric, which captures the EE of individual UEs in the previous subsection. The WSEE is given by

$$\begin{aligned} \text{WSEE} &= \sum_{k=1}^K w_k \cdot EE_k \\ &= B \left(1 - \frac{\tau_p}{\tau_c}\right) \cdot \sum_{k=1}^K w_k \cdot \frac{\log_2 \left(1 + \text{SINR}_k^{\text{ul}}\right)}{P_k}, \end{aligned} \quad (18)$$

where  $w_k$  represents the weight assigned to UE  $k$ . The weight vector  $\mathbf{w}$  can be adjusted to suit the unique characteristics of the UEs and the specific requirements of the network. This flexibility enables the WSEE to be tailored and optimized for a variety of scenarios. As will be shown later in Section VI, this metric allows for comprehensive evaluations of uplink EE under various network scenarios.

### C. Weighted-Global Energy Efficiency

A straightforward metric for comparing WSEE is the weighted-global energy efficiency (WGEE), which is defined

---

### Algorithm 1 Dinkelbach-like algorithm for WSEE maximization

---

- 1: **Input:**  $\mathbf{w}$ , tolerance  $\varepsilon$  and  $\text{max\_iter}$
  - 2: **Initialize**
  - 3:   1)  $\mathbf{q}^{(0)}$  and  $\mathbf{U}^{(0)}$  to feasible values
  - 4:   2) Set  $i = 0$ ,  $\text{WSEE}^{(0)} = 0$
  - 5: **repeat**
  - 6:   Update  $\mathbf{U}^{(i+1)} \leftarrow \mathbf{U}^{(i)}$  for fixed  $\mathbf{q}^{(i)}$
  - 7:   Update  $\mathbf{t}$  by (22)
  - 8:   Solve  $P_{\text{Dink}}^1$  and update  $\mathbf{q}^{(i+1)} \leftarrow \mathbf{q}^{(i)}$
  - 9:   Calculate  $\text{WSEE}^{(i+1)}$  w.r.t  $\mathbf{w}$ ,  $\mathbf{q}^{(i+1)}$  and  $\mathbf{U}^{(i+1)}$
  - 10:    $i \leftarrow i + 1$
  - 11: **until**  $\text{WSEE}^{(i+1)} - \text{WSEE}^{(i)} < \varepsilon$  or  $i = \text{max\_iter}$
  - 12: **Output:** last updated  $\mathbf{q}$ ,  $\mathbf{U}$  and  $\text{WSEE}$
- 

as the weighted-sum rate (WSR) divided by the total power consumption. WGEE is given by

$$\begin{aligned} \text{WGEE} &= \frac{\sum_{k=1}^K w_k \cdot SE_k}{\sum_{k=1}^K P_k} \\ &= B \left(1 - \frac{\tau_p}{\tau_c}\right) \cdot \frac{\sum_{k=1}^K w_k \log_2 \left(1 + \text{SINR}_k^{\text{ul}}\right)}{\sum_{k=1}^K P_k}, \end{aligned} \quad (19)$$

This formulation presents WGEE as a single-ratio measure, similar to the conventional global energy efficiency (GEE). In line with WSEE, an appropriate weight vector  $\mathbf{w}$  can be selected based on the specific characteristics and requirements of both the UEs and the network. Even when WSEE and WGEE use the same  $\mathbf{w}$ , the resulting values are not directly comparable. Instead, the EE of individual UEs should be recalculated based on  $\mathbf{q}$  and  $\mathbf{U}$ , which maximize WSEE and WGEE, respectively. The network's performance can then be assessed by comparing these values.

## IV. ENERGY EFFICIENCY MAXIMIZATION

### A. WSEE Maximization

The objective of this study is to maximize the WSEE by determining the optimal transmit power  $\mathbf{q}$  and LSFD combiner  $\mathbf{U}$  for each UE, while accounting for maximum transmit power, data rate requirements, and associated weights. This can be formulated as follows.

$$P_1 : \underset{\mathbf{q}, \mathbf{U}}{\text{maximize}} \quad \text{WSEE}(\mathbf{w}, \mathbf{q}, \mathbf{U}) \quad (20a)$$

$$\text{subject to} \quad \|\mathbf{u}_k\| = 1, \quad \forall k, \quad (20b)$$

$$\text{SE}_k(\mathbf{q}, \mathbf{u}_k) \geq r_k, \quad \forall k, \quad (20c)$$

$$0 \leq q_k \leq p_{\text{max},k}, \quad \forall k. \quad (20d)$$

---


$$\begin{aligned} \text{SINR}_k^{\text{ul}} &= \frac{q_k \left| \mathbf{u}_k^H \mathbb{E} \left\{ \hat{\mathbf{g}}_{mk}^H \mathbf{D}_{mk} \mathbf{g}_{mk} \right\} \right|^2}{\mathbf{u}_k^H \left( \sum_{k' \neq k} q_{k'} \mathbb{E} \left\{ \left| \hat{\mathbf{g}}_{mk}^H \mathbf{D}_{mk} \mathbf{g}_{mk'} \right|^2 \right\} + \sigma_{\text{ul}}^2 \text{diag} \left( \mathbb{E} \left\{ \left| \hat{\mathbf{g}}_{1k}^H \mathbf{D}_{1k} \right|^2 \right\}, \dots, \mathbb{E} \left\{ \left| \hat{\mathbf{g}}_{Mk}^H \mathbf{D}_{Mk} \right|^2 \right\} \right) \right) \mathbf{u}_k} \\ &= \frac{q_k \left| \sum_{m \in \mathcal{M}_k} u_{mk}^\dagger \gamma_{mk} \right|^2}{\sum_{k'} q_{k'} \sum_{m \in \mathcal{M}_k} |u_{mk}|^2 \beta_{mk'} \gamma_{mk} + \frac{1}{N} \sum_{k' \in \mathcal{P}_k \setminus \{k\}} q_{k'} \left| \sum_{m \in \mathcal{M}_k} u_{mk}^\dagger \gamma_{mk} \sqrt{\frac{\rho_{k'}}{\rho_k} \frac{\beta_{mk'}}{\beta_{mk}}} \right|^2 + \frac{1}{N^2} \sigma_{\text{ul}}^2 \sum_{m \in \mathcal{M}_k} |u_{mk}|^2 \gamma_{mk}} \end{aligned} \quad (11)$$


---


$$\quad (12)$$

---

**Algorithm 2** Nested-QT based algorithm for WSEE maximization
 

---

```

1: Input:  $\mathbf{w}$ , tolerance  $\varepsilon$  and  $max\_iter$ 
2: Initialize
3:   1)  $\mathbf{q}^{(0)}$  and  $\mathbf{U}^{(0)}$  to feasible values
4:   2) Set  $i = 0$ ,  $WSEE^{(0)} = 0$ 
5: repeat
6:   Update  $\mathbf{U}^{(i+1)} \leftarrow \mathbf{U}^{(i)}$  for fixed  $\mathbf{q}^{(i)}$ 
7:   Update  $\mathbf{z}$  by (24)
8:   Update  $\mathbf{y}$  by (28)
9:   Solve  $P_{\text{nested-QT}}$  for fixed  $\mathbf{U}^{(i+1)}$  and update  $\mathbf{q}^{(i+1)} \leftarrow \mathbf{q}^{(i)}$ 
10:  Return  $WSEE^{(i+1)}$  w.r.t  $\mathbf{w}$ ,  $\mathbf{q}^{(i+1)}$  and  $\mathbf{U}^{(i+1)}$ 
11:   $i \leftarrow i + 1$ 
12: until  $WSEE^{(i+1)} - WSEE^{(i)} < \varepsilon$  or  $i = max\_iter$ 
13: Output: last updated  $\mathbf{q}$ ,  $\mathbf{U}$  and  $WSEE$ 

```

---

Note that solving the problem  $P_1$  directly is challenging since the objective is highly non-concave jointly with respect to  $\mathbf{q}$  and  $\mathbf{U}$ . To handle this, we employ an AO approach, which separates the original problem into two subproblems that alternately optimize  $\mathbf{q}$  and  $\mathbf{U}$ . In the  $\mathbf{U}$ -subproblem, with  $\mathbf{q}$  fixed, the optimal  $\mathbf{U}$  is determined using (13). In the  $\mathbf{q}$ -subproblem, with  $\mathbf{U}$  fixed, the optimization problem for  $\mathbf{q}$  is solved to maximize the WSEE. However, even with AO, finding the optimal  $\mathbf{q}$  in the  $\mathbf{q}$ -subproblem is challenging due to the fractional form of the EE itself.

The Dinkelbach transform is widely known as an iterative method for solving single-ratio FP by decoupling the numerator and denominator [24]. For multiple-ratio objects such as WSEE in  $P_1$ , Dinkelbach-like transform can be applied by individually transforming each fraction with the Dinkelbach method [25].

$$P_{\text{Dink}}^1 : \underset{\mathbf{q}, \mathbf{U}, \mathbf{t}}{\text{maximize}} \quad \sum_{k=1}^K w_k (\text{SE}_k - t_k P_k) \quad (21a)$$

$$\text{subject to} \quad (20b) - (20d), \quad (21b)$$

$$\mathbf{t} \in \mathbb{C}^K. \quad (21c)$$

In  $P_{\text{Dink}}^1$ , the auxiliary variable  $\mathbf{t}$  is updated through the following expression.

$$t_k^* = \frac{\log_2 \left( 1 + \text{SINR}_k^{\text{ul}}(\mathbf{q}, \mathbf{U}) \right)}{P_k(\mathbf{q})}, \quad \forall k. \quad (22)$$

The iterative algorithm for solving  $P_{\text{Dink}}^1$  is provided in Algorithm 1. However, this classical transformation has a limitation that the optimized objective value of the transformed problem may not be equivalent to the original FP objective value. Thus, applying the Dinkelbach transformation individually to each ratio in multiple ratio FPs, such as WSEE, where the power of one UE affects the EE of all UE, can significantly degrade the expected performance. Also, it is known that the Dinkelbach-like transform generally fails to converge even for the simplest forms of multiple-ratio problems.

To deal with these problems, QT has been proposed to ensure that the transformed problem retains the same objective value as the original [26]. In addition, QT ensures the

equivalence to the optimal solution of the original problem, even when the target of multiple ratio FP is a monotonically increasing function  $f(x)$  of individual ratios. In QT, each single ratio  $A(\mathbf{x})/B(\mathbf{x})$  of the original objective function is transformed to  $2\lambda\sqrt{A(\mathbf{x})} - \lambda^2 B(\mathbf{x})$  with respect to the auxiliary variable  $\lambda$ . During the optimization process,  $\lambda$  is updated sequentially with the equation  $\lambda^* = \sqrt{A(\mathbf{x})/B(\mathbf{x})}$  for a fixed  $\mathbf{x}$  from the previous step.

In the case of WSEE maximization, every  $\text{EE}_k$  is in the form of single ratio. Also,  $\text{SE}_k$  is in the form of  $\log_2(1 + \text{SINR}_k^{\text{ul}})$ , where  $\text{SINR}_k^{\text{ul}}$  itself is a single ratio. Since both weighted summation with non-negative weights and  $\log_2(1+x)$  are monotonically increasing functions, successive applications of QT to  $\text{EE}_k$  and  $\text{SINR}_k^{\text{ul}}$  maintain equivalence with the original problem. First, we can reformulate problem  $P_1$  using QT for each  $\text{EE}_k$  as follows.

$$P_{QT} : \underset{\mathbf{q}, \mathbf{U}, \mathbf{y}}{\text{maximize}} \quad \sum_{k=1}^K w_k \cdot \mathcal{F}_k(\mathbf{q}, \mathbf{U}, \mathbf{y}) \quad (23a)$$

$$\text{subject to} \quad (20b) - (20d), \quad (23b)$$

$$\mathbf{y} \in \mathbb{C}^K. \quad (23c)$$

The function  $\mathcal{F}_k(\mathbf{q}, \mathbf{U}, \mathbf{y})$  in the objective of  $P_{QT}$  is derived by applying the QT to  $\text{EE}_k$ . It is expressed as (26) at the bottom of the next page. The element  $y_k$  of the auxiliary vector  $\mathbf{y} = [y_1, y_2, \dots, y_K]$  is used for optimizing  $\text{EE}_k$  and is iteratively updated for fixed  $\mathbf{q}$  and  $\mathbf{U}$ , as shown below.

$$y_k^* = \frac{\sqrt{\log_2 \left( 1 + \text{SINR}_k^{\text{ul}}(\mathbf{q}, \mathbf{U}) \right)}}{P_k(\mathbf{q})}, \quad \forall k. \quad (24)$$

Next, by applying QT once more to the  $\text{SINR}_k^{\text{ul}}$  of  $\mathcal{F}_k(\mathbf{q}, \mathbf{U}, \mathbf{y})$ , we can finally transform the original WSEE maximization problem into a tractable form as follows.

$$P_{\text{nested-QT}} : \underset{\mathbf{q}, \mathbf{U}, \mathbf{y}, \mathbf{z}}{\text{maximize}} \quad \sum_{k=1}^K w_k \cdot \mathcal{G}_k(\mathbf{q}, \mathbf{U}, \mathbf{y}, \mathbf{z}) \quad (25a)$$

$$\text{subject to} \quad (23b), (23c), \quad (25b)$$

$$\mathbf{z} \in \mathbb{C}^K. \quad (25c)$$

The function  $\mathcal{G}_k(\mathbf{q}, \mathbf{U}, \mathbf{y}, \mathbf{z})$  in the objective of  $P_{\text{nested-QT}}$  is derived by applying the QT to both  $\text{EE}_k$  and  $\text{SINR}_k^{\text{ul}}$ . It is expressed as (27) at the bottom of the next page. Similar to  $\mathbf{y}$ , the element  $z_k$  of the auxiliary vector  $\mathbf{z} = [z_1, z_2, \dots, z_K]$  is used for optimizing  $\text{SINR}_k^{\text{ul}}$ , and it is given by

$$z_k^* = \frac{\sqrt{\text{SINR}_{\text{num},k}^{\text{ul}}(\mathbf{q}, \mathbf{U})}}{\text{SINR}_{\text{denom},k}^{\text{ul}}(\mathbf{q}, \mathbf{U})}, \quad \forall k \quad (28)$$

where  $\text{SINR}_{\text{num},k}^{\text{ul}}$  and  $\text{SINR}_{\text{denom},k}^{\text{ul}}$  represent the numerator and denominator of  $\text{SINR}_k^{\text{ul}}$ , respectively. This element is iteratively updated using (28) for fixed  $\mathbf{q}$  and  $\mathbf{U}$ . Note that the objective function of the transformed  $P_{\text{nested-QT}}$  is concave with respect to  $\mathbf{q}$  as stated in the following proposition.

**Proposition 1.** *The differentiable function  $\mathcal{G}_k(\mathbf{q}, \mathbf{U}, \mathbf{y}, \mathbf{z})$  is concave with respect to  $\mathbf{q}$  when  $\mathbf{U}$ ,  $\mathbf{y}$ , and  $\mathbf{z}$  are fixed.*

---

**Algorithm 3** Dinkelbach algorithm for WGEE maximization

---

```

1: Input:  $\mathbf{w}$ , tolerance  $\varepsilon$  and  $\text{max\_iter}$ 
2: Initialize
3:   1)  $\mathbf{q}^{(0)}$  and  $\mathbf{U}^{(0)}$  to feasible values
4:   2) Set  $i = 0$ ,  $\text{WGEE}^{(0)} = 0$ 
5: repeat
6:   Update  $\mathbf{U}^{(i+1)} \leftarrow \mathbf{U}^{(i)}$  for  $\mathbf{q}^{(i)}$ 
7:   Update  $\mathbf{s}$  by (22)
8:   Solve  $P_{\text{Dink}}^2$  and update  $\mathbf{q}^{(i+1)} \leftarrow \mathbf{q}^{(i)}$ 
9:   Calculate WGEE w.r.t  $\mathbf{w}$ ,  $\mathbf{q}$  and  $\mathbf{U}$ 
10:   $i \leftarrow i + 1$ 
11: until  $\text{WGEE}^{(i+1)} - \text{WGEE}^{(i)} < \varepsilon$  or  $i = \text{max\_iter}$ 
12: Output: last updated  $\mathbf{q}$ ,  $\mathbf{U}$  and WGEE

```

---

*Proof.* The proof is provided in Appendix A. ■

Now we can apply the AO approach to maximize the WSEE after transforming it into  $P_{\text{nested-QT}}$  as in (25), by optimizing  $\mathbf{q}$  and  $\mathbf{U}$  iteratively. First, the optimal LSFD combiner  $\mathbf{U}$  is calculated for a given transmit power  $\mathbf{q}$ . Then, with the updated power and LSFD combiner, the auxiliary variables  $\mathbf{y}$  and  $\mathbf{z}$  are updated. Based on them, the problem  $P_{\text{nested-QT}}$  is solved to update the WSEE value. These steps are repeated until the WSEE value converges, yielding the optimized  $\mathbf{q}$ ,  $\mathbf{U}$ , and the optimized value of WSEE. The procedure described above is summarized in Algorithm 2.

In the  $\mathbf{q}$ -subproblem, the constraint set is convex, except for (20c). This non-convex constraint can be reformulated as

$$\text{SINR}_k^{\text{ul}}(\mathbf{q}, \mathbf{U}) \geq 2^{\frac{\tau_c}{\tau_c - \tau_p} r_k} - 1. \quad (29)$$

The numerator and denominator of  $\text{SINR}_k^{\text{ul}}$  can now be separated and expressed as follows.

$$\text{SINR}_{\text{num},k}^{\text{ul}}(\mathbf{q}, \mathbf{U}) - (2^{\frac{\tau_c}{\tau_c - \tau_p} r_k} - 1) \cdot \text{SINR}_{\text{denom},k}^{\text{ul}}(\mathbf{q}, \mathbf{U}) \geq 0. \quad (30)$$

With this reformulation, the constraint becomes a convex constraint with respect to  $\mathbf{q}$  for a fixed  $\mathbf{U}$ , as both  $\text{SINR}_{\text{num},k}^{\text{ul}}$  and  $\text{SINR}_{\text{denom},k}^{\text{ul}}$  are affine in  $\mathbf{q}$ . Therefore, replacing the minimum rate constraint in  $P_{\text{nested-QT}}$  with (30) ensures that the  $\mathbf{q}$ -subproblem is concave, as guaranteed by Proposition 1.

### B. WGEE Maximization

Like WSEE, WGEE can also be maximized by optimizing  $\mathbf{q}$  and  $\mathbf{U}$ , given each UE's maximum transmit power, data

rate requirement, and corresponding weight. The maximization problem of WGEE is as follows.

$$P_2 : \underset{\mathbf{q}, \mathbf{U}}{\text{maximize}} \quad \text{WGEE}(\mathbf{w}, \mathbf{q}, \mathbf{U}) \quad (31a)$$

$$\text{subject to} \quad \|\mathbf{u}_k\| = 1, \quad \forall k, \quad (31b)$$

$$\text{SE}_k(\mathbf{q}, \mathbf{u}_k) \geq r_k, \quad \forall k, \quad (31c)$$

$$0 \leq q_k \leq p_{\max,k}, \quad \forall k. \quad (31d)$$

Similar to  $P_1$ , (31c) can be replaced by (30). However, unlike  $P_{\text{nested-QT}}$ , where the concavity of the objective function in the  $\mathbf{q}$ -subproblem is guaranteed by Proposition 1, the WGEE cannot be transformed into a concave form with respect to  $\mathbf{q}$ , even with repeated applications of QT. Instead,  $P_2$  can be reformulated by applying the straightforward extension of Dinkelbach transform,

$$P_{\text{Dink}}^2 : \underset{\mathbf{q}, \mathbf{U}, \mathbf{s}}{\text{maximize}} \quad \sum_{k=1}^K w_k \text{SE}_k - s_k \sum_{k=1}^K P_k \quad (32a)$$

$$\text{subject to} \quad (31b) - (31d), \quad (32b)$$

$$\mathbf{s} \in \mathbb{C}^K, \quad (32c)$$

where the element  $s_k$  of the auxiliary vector  $\mathbf{s} = [s_1, s_2, \dots, s_K]$  is updated through

$$s_k^* = \frac{\sum_{k=1}^K w_k \text{SE}_k(\mathbf{q}, \mathbf{U})}{\sum_{k=1}^K P_k(\mathbf{q})}, \quad \forall k. \quad (33)$$

The iterative algorithm to solve  $P_{\text{Dink}}^2$  is presented in Algorithm 3.

Referring to (32a), it becomes evident that optimizing WGEE is closely associated with maximizing WSR. Consequently, in the optimization of  $P_{\text{Dink}}^2$ , alternative approaches, such as the weighted minimum mean square error (WMMSE) method [31], commonly employed for WSR maximization, or the Lagrangian dual form of QT, could be considered instead of Algorithm 3. However, directly applying WMMSE or the Lagrangian dual form of QT to our problem poses challenges, as these methods typically do not account for QoS constraints. In Section VI, we use these methods as benchmarks for optimization algorithms in scenarios that do not involve QoS considerations.

### C. Convergence Analysis

In the proposed Algorithm 2, the nested-QT transform with power control and LSFD combiner in an AO is guaranteed to converge to a local optimum. To prove this, we can revisit the Proposition 1. From the result of Proposition 1, one

---


$$\mathcal{F}_k(\mathbf{q}, \mathbf{U}, \mathbf{y}) = 2y_k \left( \log_2 \left( 1 + \text{SINR}_k^{\text{ul}}(\mathbf{q}, \mathbf{U}) \right) \right)^{\frac{1}{2}} - y_k^2 P_k(\mathbf{q}) \quad (26)$$

$$\mathcal{G}_k(\mathbf{q}, \mathbf{U}, \mathbf{y}, \mathbf{z}) = 2y_k \left( \log_2 \left( 1 + 2z_k \left( \text{SINR}_{\text{num},k}^{\text{ul}}(\mathbf{q}, \mathbf{U}) \right)^{\frac{1}{2}} - z_k^2 \cdot \text{SINR}_{\text{denom},k}^{\text{ul}}(\mathbf{q}, \mathbf{U}) \right) \right)^{\frac{1}{2}} - y_k^2 P_k(\mathbf{q}) \quad (27)$$

can express that  $\mathcal{G}_k$  is monotonically non-decreasing at each iteration as follows:

$$\begin{aligned}
& \mathcal{G}_k(\mathbf{q}^{(i+1)}, \mathbf{U}^{(i+1)}, \mathbf{y}^{(i+1)}, \mathbf{z}^{(i+1)}) \\
& \stackrel{(a)}{\geq} \mathcal{G}_k(\mathbf{q}^{(i)}, \mathbf{U}^{(i+1)}, \mathbf{y}^{(i+1)}, \mathbf{z}^{(i+1)}) \\
& \stackrel{(b)}{\geq} \mathcal{G}_k(\mathbf{q}^{(i)}, \mathbf{U}^{(i+1)}, \mathbf{y}^{(i)}, \mathbf{z}^{(i+1)}) \\
& \stackrel{(c)}{\geq} \mathcal{G}_k(\mathbf{q}^{(i)}, \mathbf{U}^{(i+1)}, \mathbf{y}^{(i)}, \mathbf{z}^{(i)}) \\
& \stackrel{(d)}{\geq} \mathcal{G}_k(\mathbf{q}^{(i)}, \mathbf{U}^{(i)}, \mathbf{y}^{(i)}, \mathbf{z}^{(i)})
\end{aligned} \tag{34}$$

where (a) is achieved by applying a CVX solver to satisfy the Karush-Kuhn-Tucker (KKT) condition during the update process of  $\mathbf{q}$ , because  $\mathcal{G}_k(\mathbf{q} \mid \mathbf{U}, \mathbf{y}, \mathbf{z})$  and also  $\mathbf{q}$ -subproblem are concave in  $\mathbf{q}$ ; (b) and (c) hold due to the concavity property of the auxiliary variable introduced when applying QT [26]; (d) follows from the fact that the update process of  $\mathbf{U}$  is equivalent to solving a generalized eigenvalue problem, which always attains the global optimum for fixed  $\mathbf{q}$ ,  $\mathbf{y}$ , and  $\mathbf{z}$ .

From (34), it can be seen that the weighted sum of  $\mathcal{G}_k$  is also monotonically non-decreasing at each iteration. Since the objective function value is monotonically non-decreasing and there is an upper bound due to the power constraint, the local convergence of Algorithm 2 is guaranteed [32]. On the other hand, the Dinkelbach-like algorithm used in Algorithms 1 and 3 does not theoretically guarantee local convergence even for the simplest form of multiple-ratio FP [13]. The experimental convergence of these algorithms is verified through the results presented in Section VI.

## V. COMPUTATIONAL COMPLEXITY

This section analyzes the computational complexity of the three algorithms proposed earlier. Algorithms 1–3 adopt an AO approach, where a generalized eigenvalue problem and concave sub-problems are solved iteratively. The key determinant in solving the generalized eigenvalue problem lies in computing the inverse of the  $M \times M$  matrix for each of the  $K$  UEs, which incurs a complexity of  $\mathcal{O}(KM^3)$ . The power control sub-problem, derived after applying either the Dinkelbach transform or the quadratic transform (QT), is solved using the interior point method embedded in a CVX solver [33]. Given that the system has  $K$  UEs, the computational cost of solving the KKT conditions once is  $\mathcal{O}(K^3)$ . Furthermore, the number of iterations required for the CVX solver to achieve an inner tolerance  $\epsilon_{\text{in}}$  is  $\mathcal{O}(\sqrt{K} \log(1/\epsilon_{\text{in}}))$ . To satisfy an overall accuracy of  $\epsilon_{\text{out}}$ , the number of AO iterations is given by  $I_{\text{iter}} = \mathcal{O}(\log(1/\epsilon_{\text{out}}))$ . Consequently, the total computational complexity of each algorithm is  $\mathcal{O}(I_{\text{iter}}(KM^3 + K^{3.5} \log(1/\epsilon_{\text{in}})))$  [34].

Although all three algorithms share the same computational complexity in terms of big-O notation, their actual runtime differs. Unlike the Dinkelbach transform, which solves a linear problem for the auxiliary variable, QT reformulates the numerator and denominator of the objective function into a quadratic surrogate with respect to the auxiliary variable. As a result, the number of outer iterations  $I_{\text{iter}}$  required to solve the power control sub-problem is higher for QT than for the Dinkelbach transform. In practice, the convergence

TABLE I: Parameter values for simulations

Parameter	Value
System size, $D$	1km
Bandwidth, $B$	20MHz
Carrier frequency, $f_0$	1.9GHz
Noise figure	7dB
AP selection threshold, $\delta$	0.99
PA efficiency, $\zeta$	0.4
Max. power for high-priority UE, $\rho_p^{\text{high}}, p_{max}^{\text{high}}$	0.5W
Max. power for low-priority UE, $\rho_p^{\text{low}}, p_{max}^{\text{low}}$	0.2W
Min. data rate for high-priority UE, $r_k^{\text{high}}$	1bps/Hz
Min. data rate for low-priority UE, $r_k^{\text{low}}$	0.5bps/Hz
Circuit power of UE, $P_{\text{CP}}$	1W
Coherence and pilot interval, $\tau_c, \tau_p$	200, 20

speed of QT is known to be slower than the superlinear convergence rate of the Dinkelbach transform [26], [35]. Therefore, in practice, Algorithm 2 with QT incurs a longer runtime compared to Algorithms 1 and 3.

## VI. NUMERICAL RESULTS

### A. Simulation Setup

In this section, we evaluate WSEE of uplink user-centric CF-mMIMO systems. In our simulations, we assume a scenario where 256 APs equipped with 4 antennas each and 16 single-antenna UEs are randomly distributed in a square area of size  $D \times D$ . The large-scale fading coefficient  $\beta_{mk}$  is modeled as

$$\beta_{mk} = \text{PL}_{mk} z_{mk}, \tag{35}$$

where  $\text{PL}_{mk}$  represents the path loss between the  $m$ -th AP and the  $k$ -th UE, and  $z_{mk}$  denotes the log-normal shadowing with a standard deviation of  $\sigma_{\text{sh}} = 8\text{dB}$ .  $\text{PL}_{mk}$  is calculated based on the three-slope model described in [30]:

$$\text{PL}_{mk} = \begin{cases} -L - 35 \log_{10}(d_{mk}), & \text{if } d_{mk} > d_1, \\ -L - 15 \log_{10}(d_1) - 20 \log_{10}(d_{mk}), & \text{if } d_0 < d_{mk} \leq d_1, \\ -L - 15 \log_{10}(d_1) - 20 \log_{10}(d_0), & \text{if } d_{mk} \leq d_0, \end{cases} \tag{36}$$

where  $L = 140.7\text{dB}$  is a constant determined by the communication environment, such as carrier frequency and antenna altitude.  $d_{mk}$  is the distance between AP  $m$  and UE  $k$ , and it is assumed to be  $d_0 = 10\text{m}$  and  $d_1 = 50\text{m}$ .

The CF-mMIMO system consists of two types of UEs with different priorities, each present in equal numbers. UEs with greater maximum transmit power and more demanding data transmission requirements are given higher priority, while UEs with smaller maximum transmit power and less stringent data needs are assigned lower priority. The system can determine each UE's weight based on its priority. We define the ratio of the higher-priority UE's weight  $w_{\text{high}}$  to the lower-priority

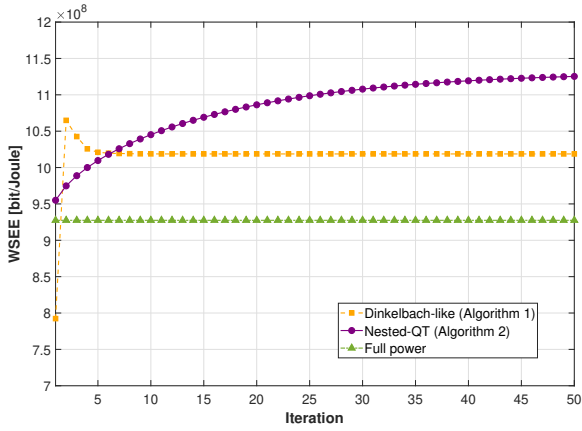


Fig. 2: The WSEE over iterations when  $\omega = 1$ .

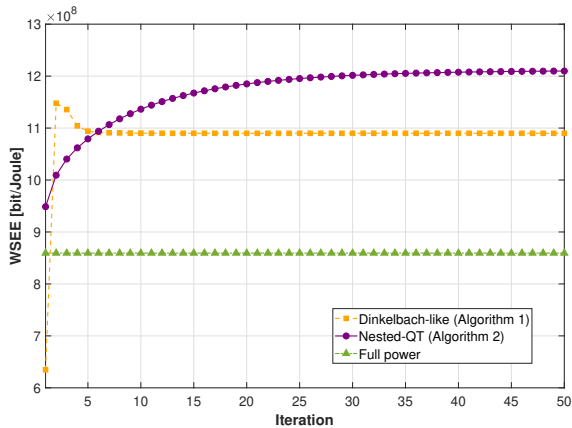


Fig. 3: The WSEE over iterations when  $\omega = 10$ .

UE's weight  $w_{\text{low}}$  as  $\omega = \frac{w_{\text{high}}}{w_{\text{low}}}$ . Additionally, to ensure a fair comparison between results using different values of  $\omega$ , the sum of all UEs' weights was normalized to be  $K$ . The values of the other parameters used in the simulation setup are summarized in Table I.

### B. Results and Discussions

Fig. 2 shows the variation in WSEE over the number of iterations when using the proposed algorithms with  $\omega = 1$ . In the figure, **Nested-QT** refers to the results from Algorithm 2. **Dinkelbach-like** represents the results of optimization using Algorithm 1. In addition, **Full power** is the result where the LSF combiner update is based on (13), but each UE uses all of its maximum transmission power without power control optimization. In the case of the **Dinkelbach-like** scheme, it was observed to converge quickly within 10 iterations, while the **Nested-QT** scheme required around 50 iterations. Compared to the **Full** scheme, the **Nested-QT** scheme achieved roughly an 18% performance improvement. In comparison with the **Dinkelbach-like** scheme, it showed about a 10% improvement at its convergence and a 5% improvement at its peak.

Fig. 3 depicts the WSEE in a scenario where  $\omega = 10$ , ensuring greater EE to higher-priority UEs. As in Fig. 2, the

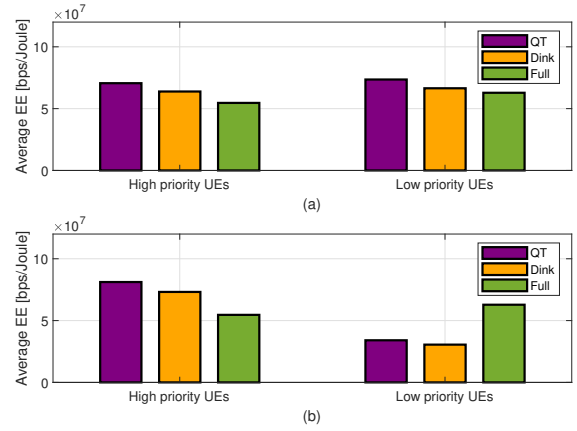


Fig. 4: Average EE according to UE priorities. (a)  $\omega = 1$ , (b)  $\omega = 10$ .

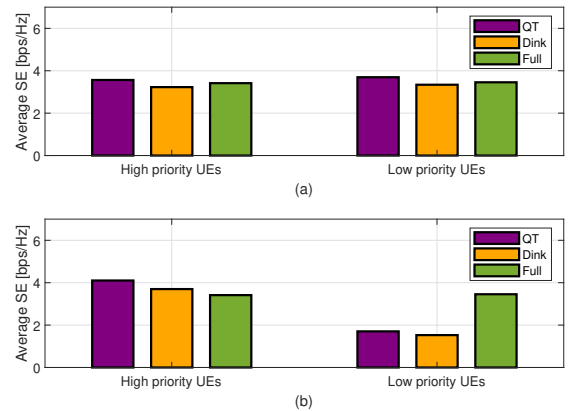


Fig. 5: Average SE according to UE priorities. (a)  $\omega = 1$ , (b)  $\omega = 10$ .

**Nested-QT** scheme achieved the best WSEE performance. A noteworthy observation in both Fig. 2 and Fig. 3 is that, with the **Dinkelbach-like** scheme, the WSEE value initially increases rapidly but then decreases at each subsequent iteration. This behavior occurs because the Dinkelbach-like transform does not guarantee an optimal solution for multiple-ratio FP problems. In contrast, the **Nested-QT** scheme is designed such that the transformed objective value always remains the same as the original and is proved to be convergent, thereby allowing a gradual approach to the solution at each iteration. Meanwhile, the **Dinkelbach-like** scheme optimizes an objective function that deviates from the original WSEE and lacks a convergence guarantee, resulting in a non-monotonic convergence pattern. As a result, directly applying the Dinkelbach-like transform can easily lead to inferior local optima and poor final performance.

The system can adjust not only the WSEE but also the performance difference between each UE group through the weights assigned to the UEs. This can be observed through the changes in the average performance of each UE group as  $\omega$  varies. Figs. 4 and 5 show the average EE and SE values for the high-priority and low-priority UE groups when  $\omega = 1$  and  $\omega = 10$ . In Fig. 4, when  $\omega$  increases from 1 to 10, the average

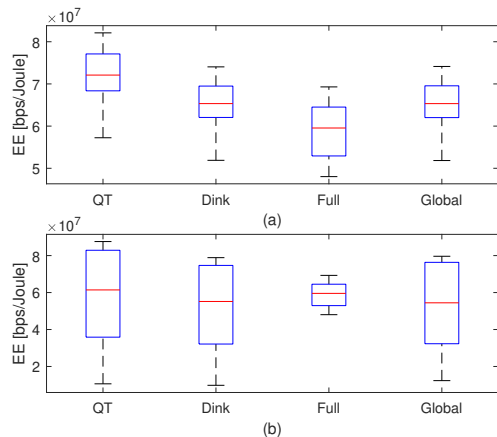


Fig. 6: EE distribution of optimization methods.  
(a)  $\omega = 1$ , (b)  $\omega = 10$ .

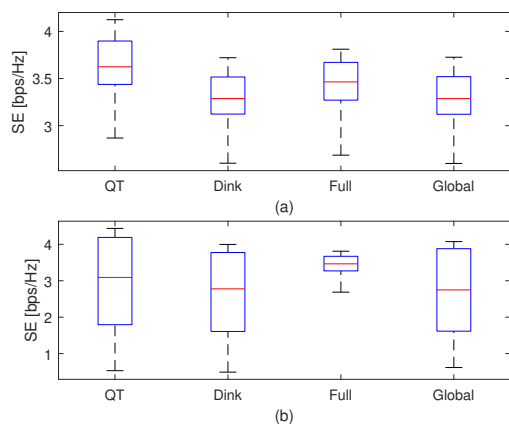


Fig. 7: SE distribution of optimization methods.  
(a)  $\omega = 1$ , (b)  $\omega = 10$ .

EE of the high-priority UE group increases, while the average EE of the low-priority UE group decreases. Thus, the system can effectively make high-priority UEs operate more energy-efficiently by assigning them higher weights. Similarly, Fig. 5 shows that as  $\omega$  increases, the average SE of the high-priority UE group rises, while the average SE of the low-priority UE group declines. In other words, UEs with higher weights not only operate more energy-efficiently but also benefit from improved data transmission rates.

Fig. 6 shows the distribution of the individual EE for each UE when maximizing WSEE and WGEE under different values of  $\omega$ , using four different schemes. **QT** is the result of using the nested-QT based approach in Algorithm 2, and **Dink** is the result of using the Dinkelbach-like approach in Algorithm 1. **Full** refers to the result in which all UEs use their maximum transmission power as in Figs. 2 and 3. **Global** is the result obtained by recalculating the EE of each UE based on the optimal transmit power and LSFD combiner obtained when WGEE is optimized using Algorithm 3. In Fig. 6(a), it is shown that **QT** achieves the best performance on average in terms of individual EE, followed by **Global** and **Dink**. The advantage of **QT** in average EE performance

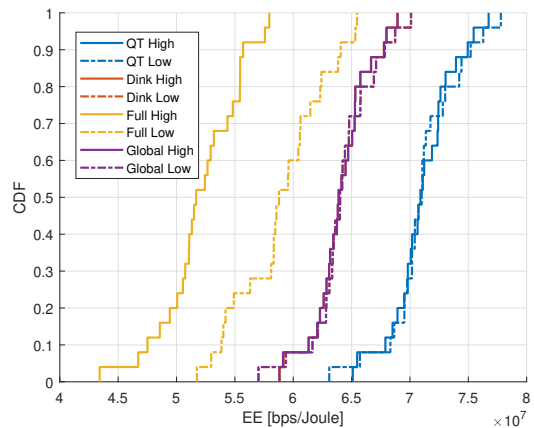


Fig. 8: CDF Plot of optimization methods and UE priorities,  
 $M = 1024$ ,  $K = 50$ ,  $\omega = 1$ .

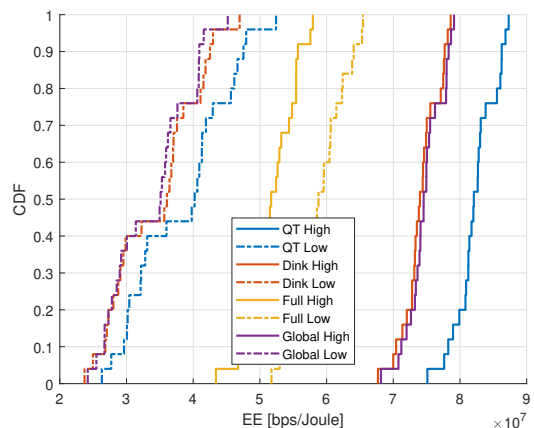


Fig. 9: CDF Plot of optimization methods and UE priorities,  
 $M = 1024$ ,  $K = 50$ ,  $\omega = 10$ .

persists even when  $\omega$  is increased to 10, as shown in Fig. 6(b). This indicates that **QT** effectively captures the individual EE impact. By comparing Fig. 6(a) and Fig. 6(b), we can observe that the distribution of EE becomes more spread across **QT**, **Dink**, and **Global**. This outcome arises because the optimization prioritizes maximizing the EE of high-priority UEs, causing the performance of low-priority UEs to converge toward a minimal threshold.

Similarly, in Fig. 7, **QT** shows the best performance in terms of average SE. The distribution of SE shows a broadening trend as  $\omega$  increases. Notably, the performance difference between **Dink** and **Global** is minimal. This indicates that applying the Dinkelbach transform to WSEE and WGEE yields only marginal differences, implying that the QT is essential for fully leveraging the characteristics of the WSEE metric.

Fig. 8 presents the CDF distribution of individual EE as the number of UEs increases to 50 and the number of APs also increased to 1024, with equal weighting for all UEs. The UEs are divided equally into 25 high-priority and 25 low-priority UEs. Consistent with prior analysis, **QT** demonstrates the most favorable EE distribution, while **Full** has the

lowest performance. The **Dink** and **Global** schemes show only minor differences. In the **Full** scheme, low-priority UEs generally outperform high-priority UEs in terms of EE, and similar trends are observed for some UEs in other schemes as well. This phenomenon, also observed in Fig. 4(a), is attributed to the significantly lower power consumption of low-priority UEs compared to high-priority UEs, creating a larger power consumption gap than the SE difference between the two UE groups. Since the weights of the two groups are equal, the lower power consumption of low-priority UEs is more advantageous in terms of EE.

Likewise, Fig. 9 presents the CDF distribution of individual EE for 50 UEs and 1024 APs with an increased  $\omega$  value of 10. First, we can confirm that the high-priority UEs achieve improved performance. While the **QT** scheme delivers the best performance, **Global** is slightly better than **Dink** but generally exhibits nearly the same results. Compared to Fig. 8, the performance of low-priority UEs has significantly decreased. All schemes except **Full—QT**, **Dink**, and **Global**—tend to guarantee only minimal performance levels for low-priority UEs, while prioritizing maximum EE for high-priority UEs. Among them, the proposed **QT** scheme consistently achieves the highest performance, regardless of UE priority.

## VII. CONCLUSIONS

We introduced and analyzed the uplink WSEE of a user-centric CF-mMIMO system, expanding beyond the conventional GEE-focused discussions in the literature. Unlike GEE-based analyses, which emphasize maximizing overall energy efficiency rather than the efficiency of individual UEs, WSEE enables an operational strategy tailored to the system's requirements, considering the characteristics and priorities of each UE. To effectively maximize WSEE, we proposed FP-based algorithms employing the Dinkelbach transform and quadratic transform. Given the complex multi-ratio nature of WSEE, the QT-based algorithm demonstrated notable performance benefits, despite its relatively slower convergence speed. Our framework offers a foundation for making system operation policy decisions that can achieve Pareto optimality, especially in systems with UEs of various capabilities and requirements. Future research could enhance the algorithm's convergence speed by modifying the closed-form of QT to function independently of the CVX solver, accommodating QoS constraints. This adjustment is expected to improve agile optimization performance, particularly in larger networks.

### APPENDIX A PROOF OF PROPOSITION 1

For notational simplicity, we drop the subscript  $k$  and represent  $\mathcal{G}(\mathbf{q}) \triangleq \mathcal{G}_k(\mathbf{q} \mid \mathbf{U}, \mathbf{y}, \mathbf{z})$  in the proof. From (27),  $\mathcal{G}(\mathbf{q})$  can be reformulated as

$$\mathcal{G}(\mathbf{q}) = 2y(\mathcal{H} \circ h)(\mathbf{q}) - y^2 P_k(\mathbf{q}). \quad (37)$$

Here, the outer function  $\mathcal{H}(x)$  and the inner function  $h(\mathbf{q})$  are defined, respectively, as follows.

$$\mathcal{H}(x) = \sqrt{\log_2(1+x)}, \quad (38)$$

$$h(\mathbf{q}) = 1 + 2z\sqrt{\text{SINR}_{\text{num},k}^{\text{ul}}(\mathbf{q})} - z^2 \cdot \text{SINR}_{\text{denom},k}^{\text{ul}}(\mathbf{q}). \quad (39)$$

Since  $P_k(\mathbf{q})$  is an affine function of  $\mathbf{q}$ , as shown in (16) and (17),  $\mathcal{G}(\mathbf{q})$  is concave with respect to  $\mathbf{q}$  if  $(\mathcal{H} \circ h)(\mathbf{q})$  is concave with respect to  $\mathbf{q}$ .

To analyze the concavity of  $\mathcal{G}(\mathbf{q})$ , we represent its second derivative as

$$\mathcal{G}''(\mathbf{q}) \propto (\mathcal{H}'' \circ h)(\mathbf{q}) \cdot (h'(\mathbf{q}))^2 + (\mathcal{H}' \circ h)(\mathbf{q}) \cdot h''(\mathbf{q}). \quad (40)$$

It can be easily verified that the first and second derivatives of  $\mathcal{H}(x)$  are always positive and negative, respectively, in its domain  $x > 0$ .

$$\mathcal{H}'(x) = \frac{1}{2(1+x)\sqrt{\log_2(1+x)}} > 0, \quad (41)$$

$$\mathcal{H}''(x) = -\frac{2\log_2(1+x) + 1}{4(1+x)^2(\log_2(1+x))^{3/2}} < 0. \quad (42)$$

In this paper, the input of  $\mathcal{H}(x)$  represents the SINR, which practically takes positive values. For  $h(\mathbf{q})$ , we have already confirmed that both  $\text{SINR}_{\text{num},k}^{\text{ul}}(\mathbf{q})$  and  $\text{SINR}_{\text{denom},k}^{\text{ul}}(\mathbf{q})$  are affine functions of  $\mathbf{q}$ . Therefore, it can be identified that if  $\sqrt{\text{SINR}_{\text{num},k}^{\text{ul}}(\mathbf{q})}$  is concave with respect to  $\mathbf{q}$ , then the entire  $h(\mathbf{q})$  is also concave with respect to  $\mathbf{q}$ . The concavity of  $\sqrt{\text{SINR}_{\text{num},k}^{\text{ul}}(\mathbf{q})}$  can be proven through the following proposition.

**Proposition 2.** *The composition of a concave function  $\phi : \mathbb{R}^{d_2} \rightarrow \mathbb{R}$  and an affine function  $f : \mathbb{R}^{d_1} \rightarrow \mathbb{R}^{d_2}$  is still a concave function.*

*Proof.* See Appendix B. ■

Since the square root function  $\sqrt{x}$  is concave for  $x > 0$  and  $\text{SINR}_{\text{num},k}^{\text{ul}}(\mathbf{q}) > 0$  is affine, it follows that the composite function  $\sqrt{\text{SINR}_{\text{num},k}^{\text{ul}}(\mathbf{q})}$  is concave with respect to  $\mathbf{q}$ . Thus,  $h(\mathbf{q})$  is concave and immediately,  $h''(\mathbf{q}) < 0$ . Returning to (40), the first term on the right-hand side is negative since it multiplies a squared term by  $\mathcal{H}'' < 0$ . The second term is also negative, as it results from the product of  $\mathcal{H}' > 0$  and  $h''(\mathbf{q})$ , which is always negative. Therefore,  $\mathcal{G}''(\mathbf{q}) < 0$ , proving that  $\mathcal{G}(\mathbf{q})$  is concave with respect to  $\mathbf{q}$ .

### APPENDIX B PROOF OF PROPOSITION 2

By the nature of the affine function, for any  $x_1, x_2 \in \mathbb{R}^{d_1}$  and  $\lambda \in [0, 1]$ , the following holds.

$$f(\lambda x_1 + (1-\lambda)x_2) = \lambda f(x_1) + (1-\lambda)f(x_2). \quad (43)$$

Now, applying the concave function  $\phi$  to (43) and using the definition of concave functions, we obtain

$$\begin{aligned} \phi(f(\lambda x_1 + (1-\lambda)x_2)) &= \phi(\lambda f(x_1) + (1-\lambda)f(x_2)) \\ &\geq \lambda \phi(f(x_1)) + (1-\lambda)\phi(f(x_2)). \end{aligned} \quad (44)$$

Rewriting the above equation gives

$$\begin{aligned} (\phi \circ f)(\lambda x_1 + (1-\lambda)x_2) &\geq \lambda(\phi \circ f)(x_1) \\ &\quad + (1-\lambda)(\phi \circ f)(x_2). \end{aligned} \quad (45)$$

By the definition of concave functions, it completes the proof that the composite function  $(\phi \circ f)(x)$  is concave for  $x$ .

## REFERENCES

- [1] W. Jiang, B. Han, M. A. Habibi, and H. D. Schotten, "The road towards 6G: A comprehensive survey," *IEEE Open Journal of the Communications Society*, vol. 2, pp. 334–366, 2021.
- [2] W. Choi and J. G. Andrews, "Downlink performance and capacity of distributed antenna systems in a multicell environment," *IEEE Transactions on Wireless Communications*, vol. 6, no. 1, pp. 69–73, Jan. 2007.
- [3] H. Q. Ngo, A. Ashikhmin, H. Yang, E. G. Larsson, and T. L. Marzetta, "Cell-free massive MIMO versus small cells," *IEEE Transactions on Wireless Communications*, vol. 16, no. 3, pp. 1834–1850, Mar. 2017.
- [4] E. Björnson and L. Sanguinetti, "Scalable cell-free massive MIMO systems," *IEEE Transactions on Communications*, vol. 68, no. 7, pp. 4247–4261, July 2020.
- [5] K. Lee, J. H. Lee, and W. Choi, "User-centric association and feedback bit allocation for FDD cell-free massive MIMO," *arXiv preprint arXiv:2405.11563*, 2024.
- [6] E. Björnson and L. Sanguinetti, "Making cell-free massive MIMO competitive with MMSE processing and centralized implementation," *IEEE Transactions on Wireless Communications*, vol. 19, no. 1, pp. 77–90, Jan. 2019.
- [7] C. Hao, T. T. Vu, H. Q. Ngo, M. N. Dao, X. Dang, C. Wang, and M. Matthaiou, "Joint user association and power control for cell-free massive MIMO," *IEEE Internet of Things Journal*, vol. 11, no. 9, pp. 15 823–15 841, May 2024.
- [8] H. D. Tuan, A. A. Nasir, H. Q. Ngo, E. Dutkiewicz, and H. V. Poor, "Scalable user rate and energy-efficiency optimization in cell-free massive MIMO," *IEEE Transactions on Communications*, vol. 70, no. 9, pp. 6050–6065, Sept. 2022.
- [9] L. You, J. Xiong, D. W. K. Ng, C. Yuen, W. Wang, and X. Gao, "Energy efficiency and spectral efficiency tradeoff in RIS-aided multiuser MIMO uplink transmission," *IEEE Transactions on Signal Processing*, vol. 69, pp. 1407–1421, 2020.
- [10] C. Isheden, Z. Chong, E. Jorswieck, and G. Fettweis, "Framework for link-level energy efficiency optimization with informed transmitter," *IEEE Transactions on Wireless Communications*, vol. 11, no. 8, pp. 2946–2957, Aug. 2012.
- [11] S.-r. Cho and W. Choi, "Energy-efficient repulsive cell activation for heterogeneous cellular networks," *IEEE Journal on Selected Areas in Communications*, vol. 31, no. 5, pp. 870–882, May 2013.
- [12] J. Zou, S. Sun, C. Masouros, Y. Cui, Y.-F. Liu, and D. W. K. Ng, "Energy-efficient beamforming design for integrated sensing and communications systems," *IEEE Transactions on Communications*, June 2024.
- [13] A. Zappone, E. Jorswieck *et al.*, "Energy efficiency in wireless networks via fractional programming theory," *Foundations and Trends® in Communications and Information Theory*, vol. 11, no. 3-4, pp. 185–396, 2015.
- [14] 3GPP, "Study on network energy savings for NR (Release 16)," 3rd Generation Partnership Project (3GPP), Tech. Rep. TR 38.864 V18.1.0, Mar. 2023. [Online]. Available: [https://www.3gpp.org/ftp/specs/archive/38\\_series/38.864/38864-i10.zip](https://www.3gpp.org/ftp/specs/archive/38_series/38.864/38864-i10.zip)
- [15] —, "Study on user equipment (UE) power saving in NR (Release 16)," 3rd Generation Partnership Project (3GPP), Tech. Rep. TR 38.840 V16.0.0, June 2019. [Online]. Available: [https://www.3gpp.org/ftp/specs/archive/38\\_series/38.840/38840-g00.zip](https://www.3gpp.org/ftp/specs/archive/38_series/38.840/38840-g00.zip)
- [16] A. Papazafeiropoulos, H. Q. Ngo, P. Kourtessis, S. Chatzinotas, and J. M. Senior, "Towards optimal energy efficiency in cell-free massive MIMO systems," *IEEE Transactions on Green Communications and Networking*, vol. 5, no. 2, pp. 816–831, June 2021.
- [17] M. Alonzo, S. Buzzi, A. Zappone, and C. D'Elia, "Energy-efficient power control in cell-free and user-centric massive MIMO at millimeter wave," *IEEE Transactions on Green Communications and Networking*, vol. 3, no. 3, pp. 651–663, Sept. 2019.
- [18] Q. Zheng, P. Zhu, J. Li, D. Wang, and X. You, "Energy efficiency enhancement in user-centric and cell-free millimeter-wave massive MIMO systems with hybrid beamforming," *IEEE Transactions on Vehicular Technology*, Apr. 2023.
- [19] R. Raghunath, B. Peng, and E. A. Jorswieck, "Energy-efficient power allocation in cell-free massive MIMO via graph neural networks," *arXiv preprint arXiv:2401.14281*, 2024.
- [20] S. Chen, J. Zhang, E. Björnson, Ö. T. Demir, and B. Ai, "Energy-efficient cell-free massive MIMO through sparse large-scale fading processing," *IEEE Transactions on Wireless Communications*, vol. 22, no. 12, pp. 9374–9389, Dec. 2023.
- [21] M. Bashar, K. Cumanan, A. G. Burr, H. Q. Ngo, E. G. Larsson, and P. Xiao, "Energy efficiency of the cell-free massive MIMO uplink with optimal uniform quantization," *IEEE Transactions on Green Communications and Networking*, vol. 3, no. 4, pp. 971–987, Jan. 2019.
- [22] T. Choi, M. Ito, I. Kanno, J. Gomez-Ponce, C. Bullard, T. Ohseki, K. Yamazaki, and A. F. Molisch, "Energy efficiency of uplink cell-free massive MIMO with transmit power control in measured propagation channel," *IEEE Open Journal of Circuits and Systems*, vol. 2, pp. 792–804, Oct. 2021.
- [23] H. Zhao, Y. Zhang, W. Xia, and H. Zhu, "Towards high energy efficiency for cell-free massive MIMO: A low-complexity approach," *IEEE Transactions on Vehicular Technology, Early Access*, vol. 73, pp. 19 907–19 912, Dec. 2024.
- [24] W. Dinkelbach, "On nonlinear fractional programming," *Management science*, vol. 13, no. 7, pp. 492–498, Mar. 1967.
- [25] R. G. Ródenas, M. L. López, and D. Verastegui, "Extensions of Dinkelbach's algorithm for solving non-linear fractional programming problems," *Top*, vol. 7, pp. 33–70, June 1999.
- [26] K. Shen and W. Yu, "Fractional programming for communication systems—Part I: Power control and beamforming," *IEEE Transactions on Signal Processing*, vol. 66, no. 10, pp. 2616–2630, May 2018.
- [27] Ö. T. Demir, E. Björnson, L. Sanguinetti *et al.*, "Foundations of user-centric cell-free massive MIMO," *Foundations and Trends® in Signal Processing*, vol. 14, no. 3-4, pp. 162–472, Jan. 2021.
- [28] B. Ghogh, F. Karray, and M. Crowley, "Eigenvalue and generalized eigenvalue problems: Tutorial," *arXiv preprint arXiv:1903.11240*, 2019.
- [29] E. Björnson, J. Hoydis, L. Sanguinetti *et al.*, "Massive MIMO networks: Spectral, energy, and hardware efficiency," *Foundations and Trends® in Signal Processing*, vol. 11, no. 3-4, pp. 154–655, Nov. 2017.
- [30] H. Q. Ngo, L.-N. Tran, T. Q. Duong, M. Matthaiou, and E. G. Larsson, "On the total energy efficiency of cell-free massive MIMO," *IEEE Transactions on Green Communications and Networking*, vol. 2, no. 1, pp. 25–39, Mar. 2017.
- [31] C. Feng, W. Shen, J. An, and L. Hanzo, "Weighted sum rate maximization of the mmWave cell-free MIMO downlink relying on hybrid precoding," *IEEE Transactions on Wireless Communications*, vol. 21, no. 4, pp. 2547–2560, Mar. 2021.
- [32] S. Boyd and L. Vandenberghe, *Convex optimization*. Cambridge university press, 2004.
- [33] M. ApS, *The MOSEK optimization toolbox for MATLAB manual. Version 10.1.*, 2024. [Online]. Available: <http://docs.mosek.com/latest/toolbox/index.html>
- [34] A. Ben-Tal and A. Nemirovski, *Lectures on modern convex optimization: analysis, algorithms, and engineering applications*. SIAM, 2001, vol. 2.
- [35] K. Shen, Z. Zhao, Y. Chen, Z. Zhang, and H. V. Cheng, "Accelerating quadratic transform and WMMSE," *IEEE Journal on Selected Areas in Communications*, Nov. 2024.